

Mixing Mechanisms in a Pair of Impinging Jets

Nasser Ashgriz*

State University of New York at Buffalo, Buffalo, New York 14260

William Brocklehurst†

SPARTA, Inc., El Segundo, California 90245

and

Douglas Talley‡

U.S. Air Force Research Laboratory, Edwards Air Force Base, California 93524-7660

An experimental investigation of mixing in impinging jet atomizers is conducted. Both miscible and immiscible liquid jets are tested. In the miscible liquid jet experiments, two water jets are impacted on each other. One of the jets is colored and traced across the spray. The liquid is sampled at different locations in the spray using a linear patternator. The volume fraction of each jet in the sampled volume is determined through the measurement of the color intensity. In the immiscible liquid jet experiments, a water–kerosene combination is used. The local volume fractions are determined by direct measurement of the volume of each component in the sampled volume. The volume fraction profiles are used to characterize the mixing processes and determine the quality (or extent) of mixing in such atomizers. Results show that two distinct processes control mixing: 1) the ability of the two jets to redirect each other on impact and before atomization (preatomization process) and 2) the turbulent dispersion in the spray region (postatomization process). The preatomization process can result in two types of atomizations: reflective and transmissive atomization. In the reflective atomization, the jets basically bounce off of each other, causing the fluid of each jet to remain on the same side of the jet. In the transmissive atomization, the direction of the momentum does not change completely, and the fluid of each jet flows to the side of the other jet. The results show that in this type of atomization, the higher the jet momentum in the plane of jet centerlines, the higher the degree of stream crossing and, therefore, the lower the extent of mixing. The directional momentum increases by increasing jet velocity and diameter and the impingement angle. On the other hand, the turbulent dispersion in the postatomization region improves the mixing. Consequently, the extent of mixing increases downstream of the impingement point.

Nomenclature

A_i	=	area of stream i
D_i	=	diameter of stream i
F	=	nominal mixture ratio, $W_2/(W_1 + W_2)$
f	=	local mixture ratio, $w_2/(w_1 + w_2)$
\hat{f}	=	local mixture ratio for points where $f > F$
L/D	=	length-to-diameter ratio of nozzles
M_i	=	momentum of stream, i
N	=	number of samples with $f < F$
\tilde{N}	=	number of samples with $f > F$
V_i	=	velocity of stream i
W	=	total nominal (input) weight flow rate of spray, $W_1 + W_2$
W_i	=	nominal or input weight flow rate of stream i
w	=	total local weight flow rate, $w_1 + w_2$
w_i	=	local weight flow rate due to stream i
x	=	minor axis of spray cross section
y	=	major axis of spray cross section
z	=	spray axis along flow direction
α	=	impingement angle
ρ_i	=	density of stream i
Φ	=	extent of mixing or mixing efficiency, $100(1 - \phi)$
ϕ	=	mixing coefficient described by Eq. (1)

I. Introduction

THE performance of a biliquid propellant rocket motor is closely coupled to the mixing and chemical reaction among the pro-

pellant or propellant combination in the combustor. To minimize the physical size of the combustion chamber, certain limitations have to be set on the residence time of the reactants in the chamber. The residence time is mainly governed by, among other parameters, the rate of mixing and chemical reaction between the propellants. Mixing itself is controlled by the quality of atomization, the mass distribution of each propellant in the spray, and the simultaneous action of the vaporization, diffusion, and turbulence. The first-order effect, however, seems to be the overall mass distribution generated by the injector.

One of the techniques for attaining efficient mixing of the liquid propellants is impinging two or more liquid jets at a common point. High-velocity jet impingement results in the simultaneous atomization and mixing of the liquid propellants. There are numerous experimental as well as theoretical studies on the mechanisms of atomization of the impinging jets. These studies^{1–13} show that when two jets collide they form a sheet in the direction perpendicular to the plane of the jets. Waves form on the surface of the sheet and grow until the sheet breaks up into small droplets. The generated spray has an elliptical cross section, with its major axis in the plane of the liquid sheet. A review by Ryan et al.¹⁰ addresses the various mechanisms that are believed to be responsible for the atomization of the impinging jets. Because the sizes of the droplets formed from the impinging jet atomizers is directly related to the thickness of the liquid sheet, several studies have focused on the variation of the thickness of the liquid sheet.^{14–16} It is generally found that the sheet thickness is inversely proportional to the radial distance from the impingement point. Two-impinging-jets mixing is also used in reaction–injection–molding processing equipment to provide good micromixing for viscous fluids.^{17–19} It is also one of the techniques used to reduce the timescale of micromixing in precipitators.²⁰ Mahajan and Kirwan²⁰ measured the concentration of the mixture after the impingement of two reacting jets (1-naphthol and diazosulfanilic acid). They provided the overall mixture concentration as a function of hydrodynamics and mixer

Received 7 August 2000; revision received 6 November 2000; accepted for publication 28 November 2000. This material is declared a work of the U.S. Government and is not subject to copyright protection in the United States.

*Professor, Department of Mechanical and Aerospace Engineering.

†Engineer, 615 Nash Street.

‡Research Scientist, Propulsion Directorate.

geometry. The spatial distribution of the mixture fraction was not provided.

Studies on the macromixing process between the two streams, however, are scarce. The available literature is mainly concerned with the development of correlations for the spatial distribution of two components of a biliquid impinging stream spray and the physical configuration of the injection system. However, no information is provided on the mechanism of the mixing between the streams. The objective of this study is to provide some understanding of the processes that are responsible for this mixing.

II. Literature Review

Rupe²¹ conducted the first comprehensive experimental investigation of the mixing in impinging jets, at the Jet Propulsion Laboratory, California Institute of Technology. Because it was difficult to use actual liquid propellants in a systematic investigation of mixing, alternative simulating fluids were utilized. These simulants were predominately immiscible liquids because the mixture ratio of the two liquids could be determined by collecting the liquid at various points in the spray and measuring the volume of the two immiscible liquids in the sample. In addition, immiscible liquids approximately duplicated the physical properties of some propellants. For instance, carbon tetrachloride and water were used to simulate a nitric acid-aniline propellant system. Nitric acid and aniline were believed to be immiscible.

The primary instrument for the measurement of the mixing in sprays in Rupe's²¹ experiments was a patternator. His patternator was composed of an array of test tubes that collect liquid samples from the spray cross section. The extent of mixing was then determined by measuring the mixture fraction of each component in each test tube. By assuming that the ideal spray was one in which the local mixture ratio was constant and equal to the input mixture ratio, and by comparing the departure of the local mixture ratio of an actual spray with that of the ideal spray, Rupe²¹ defined the following coefficient to describe the degree of mixing in the impinging injectors:

$$\phi = \sum_0^N \frac{w}{W} \left(\frac{F-f}{F} \right) + \sum_0^{\dot{N}} \frac{w}{W} \left(\frac{F-\tilde{f}}{F-1} \right) \quad (1)$$

where f and F are the local and input mixture ratios, respectively, and w and W are the total local and input weight flow rates, respectively. The percentage of this deviation represents the extent of mixing or mixing efficiency:

$$\Phi = 100(1 - \phi) \quad (2)$$

The investigators after Rupe²¹ have used this coefficient to characterize, evaluate, and compare sprays of different configurations produced under various conditions. Values of Φ measured in nonreactive systems with fully developed flows from circular jets were in the range of 50–85%. Rupe²¹ typically found maximum values between 75 and 85% near optimum conditions, and some were above this level. He concluded that, within limits ($\pm 5\%$), the mixing efficiency for a given circular orifice combination reaches a maximum when the product of the ratios of the velocity heads and stream diameters is equal to unity.

The quality of mixing has been evaluated by the determination of Φ over significant ranges of six distinct variables: 1) momentum ratio M_1/M_2 , 2) impingement angle α , 3) area ratio A_1/A_2 , 4) area scale A_1/A'_2 , 5) fluid physical properties, and 6) flow characteristics and impingement length l . The following is a general explanation of the effect of these parameters on the mixing process.

A. Effect of the Momentum Ratio

Experimental measurement of Φ for different values of momentum ratio by Rupe²¹ for a one-on-one, and Elverum and Morey²² for two-on-one, two-on-two, and four-on-one impinging jets have shown that the maximum value of Φ occurs near $M_1/M_2 = 1.0$ and that the liquid-phase mixing is relatively insensitive to momentum ratio at or near a momentum ratio of 1.0.

The experimental results^{21,22} indicate that the distribution of each component of the liquid in the plane of stream centerlines is not uniform. However, the local mixture ratio along the major axis of the spray cross section is nearly constant and equal to the nominal value (if the spray is produced by streams of equal momentum and area ratio). The mass distribution significantly changes with the momentum ratio. The maximum local mass flow shifts along the impinging plane in the direction of the high-momentum stream. As this shift takes place, the spray cross section assumes a kidney shape that is symmetrical about the impinging plane only.²¹

B. Effect of the Impingement Angle

Rupe's²¹ experimental results show a linear correlation between the impingement angle and Φ . Better mixing is obtained at lower impingement angles. This is in agreement with the actual rocket tests of Elko and Stary,²³ which show that the rocket performance increases as the impingement angle decreases from 90 to 45 deg. When the angle studies were extended to 120 deg, the actual rocket test results indicated that minimum performance is obtained for $\alpha = 90$ deg. Tests with simulants²¹ show an optimum mixing at the impingement angle of 45 deg. The impingement angle influences the mixing in two different manners. Higher impingement angles result in a higher impact-induced turbulence and, therefore, higher turbulence mixing. On the other hand, higher impingement angles allow less contact time between the liquids of the two streams.

C. Effect of the Area Ratio

The area ratio indicates the extent of interaction between the two streams. Rupe²¹ studied the area ratios 0.261–1.69 in eight steps and for $M_1/M_2 = 1.0$ and $\alpha = 60$ deg. He has reported the following results: The maximum value of Φ (and, hence, point of best mixing) occurs for momentum ratios less than 1.0 as the area ratio becomes smaller than 1.0. It has also been observed that this shift in the maximum point for a given area ratio is accompanied by an increase in the value of Φ . Considering the maximum for all area ratios, an overall maximum point apparently occurs in the region where $A_1/A_2 = 0.7$ and $M_1/M_2 = 0.81$. Based on the preceding conclusions, Rupe²¹ correlated his data from a pair of impinging streams with the ratio of the velocity heads and stream diameters, that is, $(\rho_1 V_1^2 D_1)/(\rho_2 V_2^2 D_2) = 1.0$. Elverum and Morey²² later used this equation to show that the momentum ratio has to be equal to the jet diameter ratio to have optimum mixing, that is, $M_1/M_2 = (\rho_1 V_1^2 D_1^2)/(\rho_2 V_2^2 D_2^2) = D_1/D_2$. Using the mixture ratio in this equation, they wrote the following correlation for optimum mixing:

$$(w_1/w_2)^2(\rho_2/\rho_1)(D_2/D_1)^3 = 1 \quad (3)$$

D. Effect of the Area Scale

Rupe²¹ considered nozzles with areas from 0.8 mm² ($D_i = 0.9$ mm) to 3.1 mm² ($D_i = 1.8$ mm). Based on the area of the smallest orifice of the series, these orifices provided area scale factors of 1.0, 1.75, 2.50, and 3.75. Rupe's nozzles were all provided with monotonic entries, a turbulence inducing roughed surface for approximately 5 diameters from the entry end, and a total length of about 22 orifice diameters. His mixing tests showed that a nearly linear trend existed between the mixing coefficient and the area scale. The mixing factor increased with increasing area scale. However, the changes in mixing factor were small compared with area changes. Rupe²¹ suggested that the available energy is utilized in a more efficient manner as the stream diameter increases or that the increase in kinetic energy available for mixing and/or increase in Reynolds number influences both the scale and magnitude of stream turbulence to increase mixing.

E. Effect of Other Parameters

There are several other parameters that are influential on the mixing process. Some of the more important ones are as follows.

1. Physical Properties

Changes in fluid properties influence mixing by changing the hydraulic characteristics of the orifices due to changes in Reynolds

number and by changing the stream dynamics. The physical properties of a liquid that could have an influence on the mixing include density, viscosity, surface tension, and miscibility. The influence of density on stream dynamics is basically incorporated in correlations with momentum or kinetic energy. The surface tension effect may have small influence on the mixing compared to large liquid inertia. The effect of viscosity, in addition to its effect on stream characteristics, may appear in the shear layer in the preatomization region. This effect has not been investigated.

2. Miscibility

Rupe²¹ has conducted an experiment with water–water impingement, in which he added water-soluble nigrosine dye to one of the streams. Then, using a photometric technique, he has calculated the mixing efficiency for three values of momentum ratio, that is, 0.6, 1.0, and 1.67, with an area ratio of 1.0 and impingement angle of 60 deg. His data indicate that the value of Φ for $M_1/M_2 = 1$ is higher by nearly 10% than a comparable value obtained with immiscible liquids.

3. Nozzle Characteristics

Hoehn and Rupe²⁴ and Nurick²⁵ have considered nozzles with different inlet conditions. They have found that for circular, unlike-impinging-doublet elements, the mixing uniformity decreases when sharp-edged orifices are used. They have attributed this reduction to the cavitation in the orifice. Orifices that are modified by length, entrance condition, and/or subjected to different operating conditions to prevent cavitation have resulted in higher mixing factors. Noncavitating circular orifices produce a maximum mixing factor of about 8% higher than those for the cavitating flow conditions.

McHale and Nurick^{26,27} have investigated the mixing efficiency in noncircular orifices. They have concluded that noncircular elements produce significantly better mixing efficiencies than a circular, unlike-doublet at equivalent design conditions. However, Hoehn et al.²⁸ have shown that this mixing disparity cannot necessarily be related to shape alone, nor can it be extrapolated to all noncircular orifice geometry design conditions.

4. Pattern and Number of Streams

There are several studies on various types of injectors. Elverum and Morey²² have studied mixing in two-on-one, two-on-two, and four-on-one impinging jets with circular orifices and have provided the mixing efficiency for various flow conditions. Falk and Burick,²⁹ Dickerson et al.,³⁰ and Nurick and Clapp³¹ have studied the mixing in arrays of like-impinging injectors. They have investigated the effects of fan spacing, fan inclination angle, and the fan cant angle. Ferrenberg and Jaqua³² have studied mixing in triplet, pentad, and coaxial element injectors and have provided the mixing efficiency as a function of various mixing parameters.

A review by Riebling³³ shows that the reported correlations can be expressed in the following form:

$$(A_2/A_1)_{\Phi_{\max}} = k[(\rho_1/\rho_2)F^2]^b \quad (4)$$

where constant k is a unique function of the ratio of the number of the streams of one fluid to the number of the streams of the other fluid (n_1/n_2) and b is a constant that is relatively insensitive to changes in n_1/n_2 . Repling's results show that, for a constant included impingement angle, the area ratio for maximum mixing efficiency is a function of the dimensionless grouping $(\rho_1/\rho_2)F^2$, which may, thus, play a key role in the mixing process.

5. Mixing in Hypergolic Liquids

Mixing studies with hypergolic liquids have not been very extensive because of the difficulty in measuring the mixture fraction in the highly reactive flows. These studies have mainly reported general qualitative information on the mixing. Lawver,³⁴ Houseman,³⁵ Johnson,³⁶ and Zung and White³⁷ have conducted experiments on the mixing process in the impingement of a nitrogen tetroxide jet with a hydrazine jet. They have reported two distinctively different separated flows. At low chamber pressures and for nitrogen

tetroxide temperatures above the boiling point, vaporization of the oxidizer has been significant, resulting in a gas/liquid impingement. The resulting spray pattern shows that hydrazine droplets are mainly confined to the fuel side. Photographs of the flame also show that combustion mainly occurs on the fuel side, indicating a separated flow, termed blow apart. Separated flows are also observed with liquid/liquid impingement at higher chamber pressures (above 230 psia). The resulting liquid sprays definitely show color variations with colorless hydrazine along the fuel side of the spray and brownish liquid nitrogen tetroxide on the oxide side. This indicates very poor intermixing of the droplets and ligaments of two liquid propellants. Stream mixing is observed at lower chamber pressures (less than 230 psia) and with nitrogen tetroxide temperatures below the boiling point. The sprays resulting from liquid/liquid impingement show a very uniform brownish color, indicating good intermixing of droplets and ligaments of the two propellants.

III. Experimental Apparatus and Procedure

Although the volume of the experimental data on the relationship between the impingement conditions and the quality of mixing is extensive, understanding of the mechanisms involved in the mixing process is lacking. The present experiment is aimed at improving our knowledge of the mixing process. The effects of the jet velocity, jet diameter, and impingement angle on the mixing are considered. The impingement of two miscible liquids (water–water) is studied to eliminate additional effects related to surface tension, which may arise in immiscible liquid impingement.

The experimental system consists of a flow system, an injector setup, a patternator, a diode array spectrophotometer, and the Greenfield flow visualization system. The flow system consists of a pressurization system, a holding tank, and gauges. Regulated K bottles of nitrogen are used to drive the flow. This delivers a constant pressure to two 35-liter stainless steel tanks filled with water. A red dye (food coloring) is added to one of the tanks. The steady flow is monitored by a pressure gauge. The flow rate is calibrated with a graduated cylinder and stopwatch. The precision of the gauge allows the flow rate to be set to within 0.03 ml/s of the desired flow rate, and, as a result, the jet velocity is determined to within 0.1 m/s.

Because the characteristics of the spray change with position, it is important to have the same reference point for each test. The origin of the coordinate axis, $z = 0$, for the experiment is set at the jet impingement point. The y axis is chosen to be the direction perpendicular to the incoming jets (along the major axis of the spray), and the x axis is in the same direction as the jets (along the minor axis of the spray) (see Fig. 1).

A total of five injectors are used. The injectors are either the plain-faced orifice type or long capillary needles. The three plain-faced orifices have diameters of 330, 508, and 711 μm , with orifice length to diameter ratios L/D of 1, 5.4, and 7, respectively. The two capillary needles have inner diameters of 508 and 711 μm , with

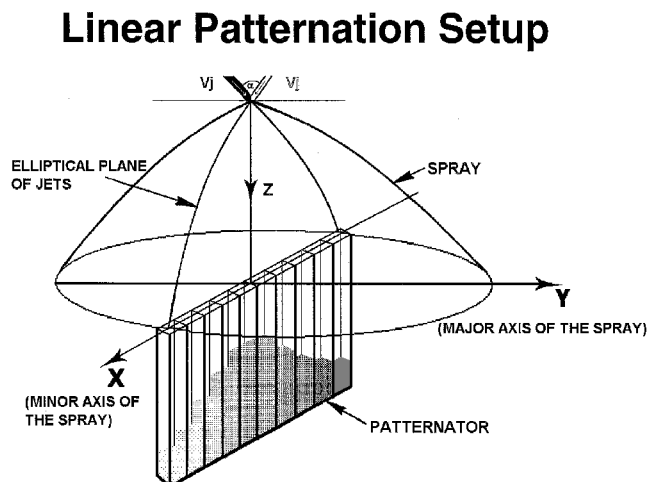


Fig. 1 Schematic diagram of spray axis and linear patternator.

L/D of 87.5 and 16, respectively. The jet velocities are in the range of 8.0–27.6 m/s.

The injectors are mounted on an assembly that allows the impingement angle and the alignment to be adjusted. Two aluminum plates with four slots milled into them hold the injector onto the spray stand. The slots are cut such that the impingement angles between the injectors can be set at 60, 90, and 120 deg. One plate is attached to a platform directly, and its position remains fixed relative to the spray stand. The second plate is screwed to a sliding table that is then attached to the same platform. This table allows the second injector to move in one direction relative to the first. A micrometer is used to adjust the position of the second injector.

Ideally, the impingement of two jets with the same diameter should result in a symmetric spray. Great care is taken to produce a symmetric spray. The jets are first aligned by sight. The patternator is then used to measure the spray at a few points, and then finer adjustments are made to make the spray symmetric. First the flow rates are adjusted so that the momentum of the two jets is equal and the spray fan is in the vertical plane. The position of the movable injector is adjusted until the fan is perpendicular to the jets. After the fine adjustments are completed, the mixing measurements are initiated. The measurements are taken at every 3.175 mm in the x direction. Data are gathered at various axial distances z from the impingement point.

A linear patternator was built by using 20 of 3.175×3.175 mm square cross-sectional brass tubing, held linearly by a fixture. One end of these tubes is used for liquid collection, and the other end is bent and put into a test tube. Before the start of each experiment the patternator is completely cleaned. A shutter is set on top of the patternator, so that the transient effects at the start and stop of the flow are eliminated. After a steady flow is achieved, the shutter is removed, and the patternator collects the liquid. The time of filling, the fluid volume, and the concentration of the dye in each test tube are measured.

The concentration of the dye is measured by an HP 8450 ultraviolet/visible (UV/VIS) spectrophotometer. This instrument passes 200–800 nm bandwidth UV/VIS radiation alternately through the sample and reference cells, twice in each 1-s measurement period. A holographic grating linearly disperses the radiation to the 200 individual diode detectors in each of the UV and VIS detector arrays for a total of 401 resolution elements. The Greenfield instrument is used to make direct visualizations of the impingement. The Greenfield instrument uses short-duration flashes generated by a xenon flash tube to capture images of droplets on a 768×493 sensor array charge-coupled device.

IV. Experimental Results

Previous studies on the mixing quality have shown that optimum mixing for circular jets with equal diameters occurs for $M_1/M_2 = 1$. Therefore, we have limited our study only to impingement of two equal diameter jets with equal velocities. The test matrix comprises combinations of collision angles of 60 and 90 deg, with jet velocities in the range of 8.0–27.6 m/s. Measurements for $V_i < 8.0$ m/s are not performed because at this test condition the two jets coalesce, and an adequate spray is not formed. For each test condition, the dye concentration and the liquid volume flux are measured only along the minor axis of the spray because the extent of mixing is best observed along this axis.

A. Stream Characteristics

The flow characteristics of the liquid streams before impingement have a significant effect on the mixing process. The streams considered here are turbulent, and their surfaces are nonsmooth and fluctuate. Depending on the nozzle configuration, the scale of fluctuations on the streams is different. For long L/D , the jets have a very steady core with small fluctuations at the jet surface. At small L/D , the core flow of the stream itself fluctuates. At even smaller L/D or at high injection velocities, the stream spreads rapidly on exiting the nozzle. The cavitation bubble inside the injector is thought to be responsible for this spreading.

Typical jet characteristics for a nozzle (capillary needle) with a $711\text{-}\mu\text{m}$ diameter and a length-to-diameter ratio of $L/D = 16$ are shown in Fig. 2 for three jet velocities of $V_i = 8, 13.5$, and 20 m/s. Direct visualization of the jet behavior reveals the following characteristics. Both large- and small-scale disturbances are observed on the surface of the jet. Small-scale disturbances appear close to the orifice, whereas large-scale disturbances are observed farther downstream. Small-scale disturbances damp out, whereas the large-scale disturbances grow along the jet axis. As the jet velocity is increased, the large-scale disturbances are delayed to a farther distance downstream of the nozzle. The frequency of the fluctuations on the jet surface increases with increasing jet velocity.

Figure 2a for $V_i = 8$ m/s shows that the jet surface only contains large-scale, low-frequency fluctuations. As the jet velocity is increased to $V_i = 20$ m/s in Fig. 2c, the jet surface close to the nozzle contains small-scale, high-frequency fluctuations, which damp farther downstream of the nozzle and transform into similar types of fluctuations as in a low-velocity jet close to the nozzle. These fluctuations arise from the previously reported helical disturbances, which result in the entire jet assuming a helical form. Hoyt and Taylor³⁸ indicated that the helical disturbances grow due to the aerodynamic form drag. This conclusion is made based on noting that a jet discharging into surrounding air moving at the same speed as the jet

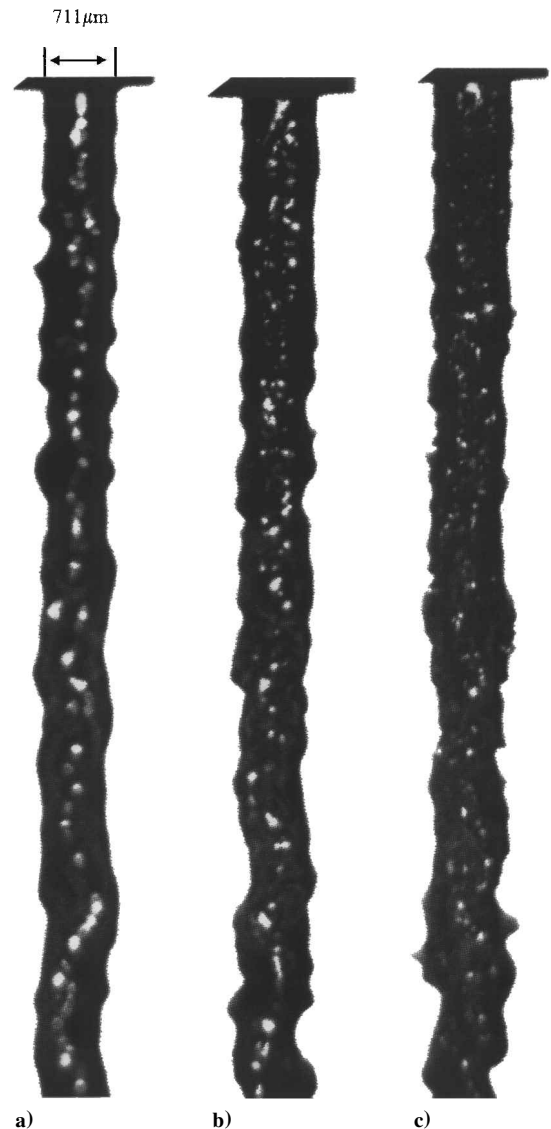


Fig. 2 Close-up images of liquid stream with jet diameter $D_j = 711 \mu\text{m}$ and at three different jet velocities: a) $V_j = 8$ m/s ($Re = 5.69 \times 10^3$), b) $V_j = 13.5$ m/s ($Re = 9.601 \times 10^3$), and c) $V_j = 20$ m/s ($Re = 1.4224 \times 10^4$).

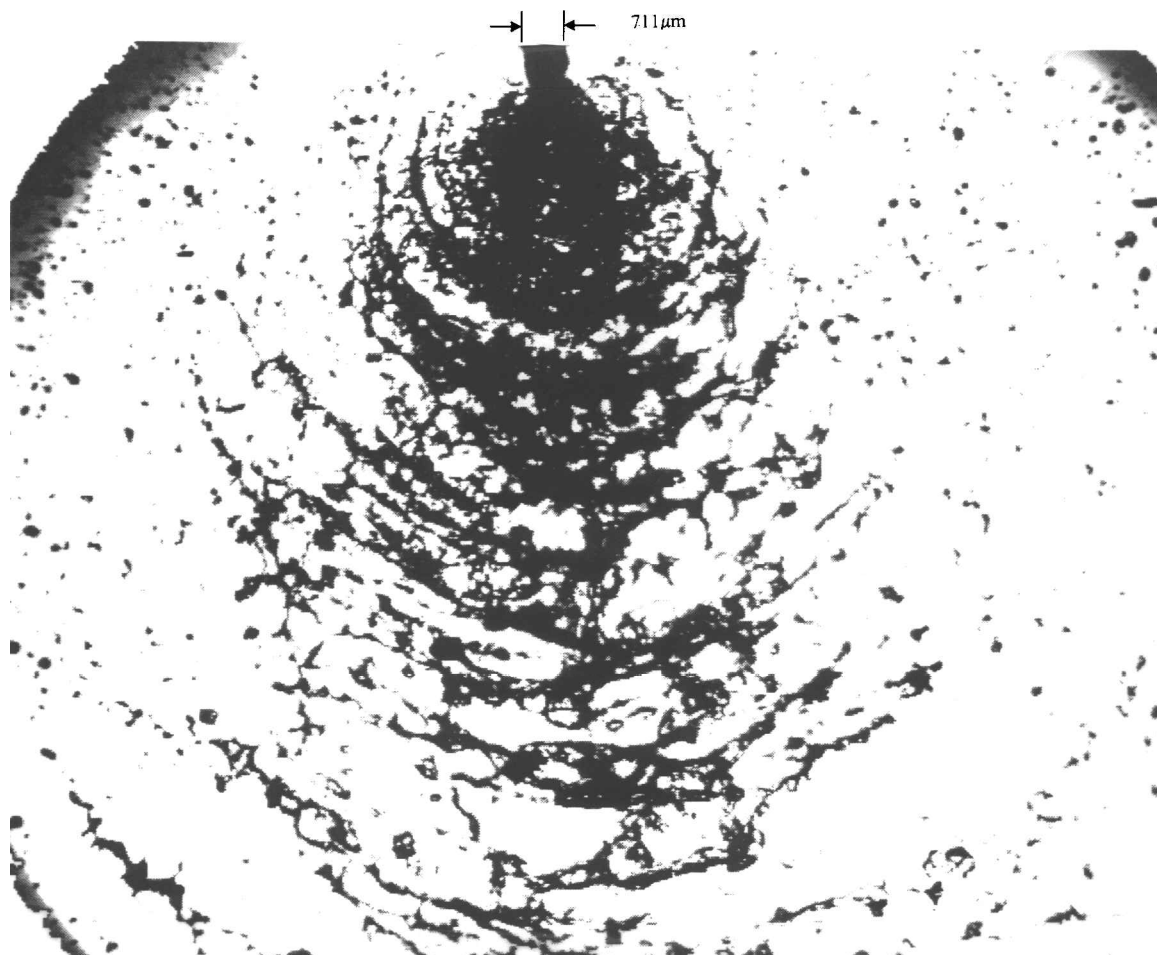


Fig. 3 Atomization of impinging doublet along spray major axis for $V_j = 20$ m/s, $D_j = 711 \mu\text{m}$, and impingement angle of 60 deg.

remains relatively stable, compared with the case when the jet is discharged into stagnant air.

Our observations of the streams indicate that for the impingement point approximately 20 diameters downstream of the nozzle the small-scale, high-frequency fluctuations are damped out and only large-scale helical disturbances control the impingement process. As the jet velocity increases, the amplitude of the low-frequency, helical disturbances at the impingement point increases. If the amplitude of the helical disturbances becomes large, they will have a significant effect on the mixing processes because they cause the two jets to not collide head-on. This results in the fluctuations of the stagnation point, which will be discussed in the next section. Finally, at small L/D and high flow velocities, a dramatic change in the jet profile is observed, where the stream spreads as it exits the nozzle. This is believed to be due to the formation of a cavitation bubble inside the injector.

B. Atomization Process

A typical image of the atomization process is presented in Fig. 3. When two jets impinge, a liquid sheet is formed in the plane perpendicular to the plane of impingement. The liquid sheet becomes unstable and breaks into liquid ligaments, which consequently break into small drops. The formation of the liquid ligaments are mainly due to the so-called impact waves, which radially propagate from the point of impingement.

The spray shown in Fig. 3 reveals that the waves are not exactly symmetric, but have a zigzag-type structure. We have observed similar zigzag-type structures on the images reported by the other investigators. This structure is due to the fluctuation of the stagnation point at the plane of impinging jets. These fluctuations are more pronounced when one observes the plane of impingement as shown

in Fig. 4 for the same conditions as in Fig. 2. Figure 4 clearly shows that as the jet velocity increases, the spreading along the minor axis (x axis) of the spray increases. This is due to an increase in the kinetic energy of the uninteracted part of the two jets, which stretches the liquid. This effect explains the observed increase in the spray angle in the plane of the impinging jets with increasing the jet velocity (discussed in the next section).

Another effect that is evident from Fig. 4 is the increase in the frequency of the observed stretches with increasing the jet velocity. As discussed, this is due to the increase in the frequency of the surface disturbances of each stream. This increase in frequency causes the impact waves to become more intermixed and harder to identify (see Fig. 3).

C. Mixing Mechanisms

The extent of mixing is measured by adding a dye (food color) to one of the jets and collecting the liquid on the impingement plane (x axis) using the linear patternator. The concentration of the dye is then measured using a spectrophotometer. Figures 5–7 show the mixture fraction on the impingement plane for three different jet diameters and several jet velocities. A very distinct feature is evident. At low jet velocities, when the two jets impinge and atomize, most of the liquid from each jet tends to stay on the same side as the original jet. The two jets seem to bounce off of each other. For instance, for $D_i = 330 \mu\text{m}$ and $V_i = 20$ m/s, in Fig. 5, the jet on the left (negative x axis) is dyed, and the mixture fraction, measured at 9.21 cm downstream of the impingement point, continuously reduces from 0.49 ± 0.02 to 0.44 ± 0.02 . The experimental error in determining the mixture ratio is less than 0.02. Therefore, a reduction of 0.05 ($0.49 - 0.44$) is greater than the experimental error and is clearly an indication of the reduction in the mixture ratio. Similar results are

Plane of Impinging Jets

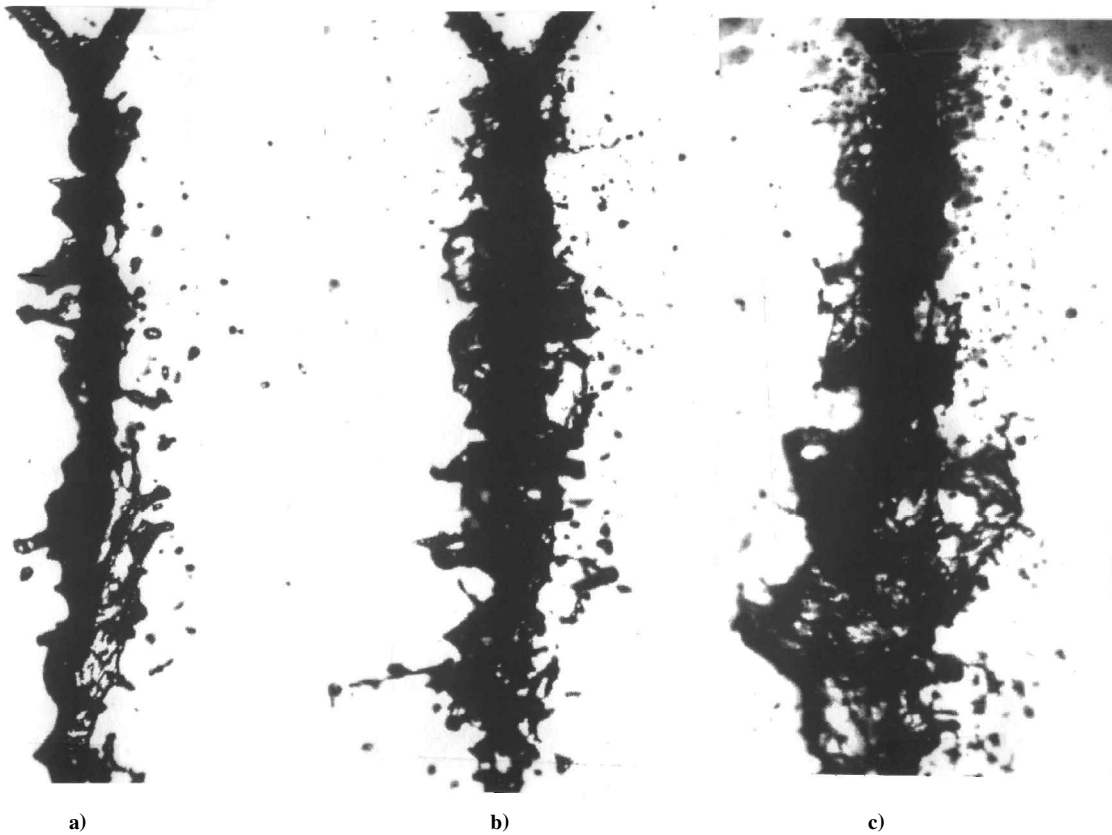


Fig. 4 Atomization of an impinging doublet along the spray minor axis for a jet diameter of $D_j = 711 \theta \text{ m}$ and for three different jet velocities: a) $V_j = 8 \text{ m/s}$ ($Re = 5.69 \times 10^3$), b) $V_j = 13.5 \text{ m/s}$ ($Re = 9.601 \times 10^3$), and c) $V_j = 20 \text{ m/s}$ ($Re = 1.4224 \times 10^4$).

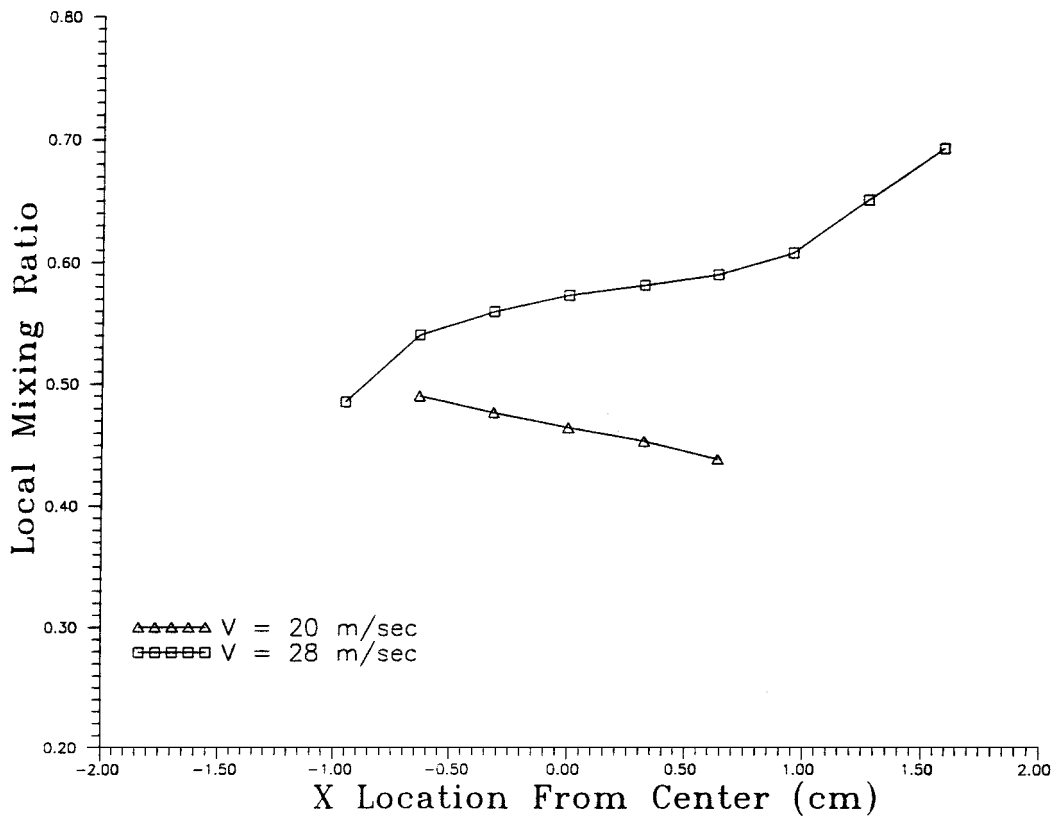
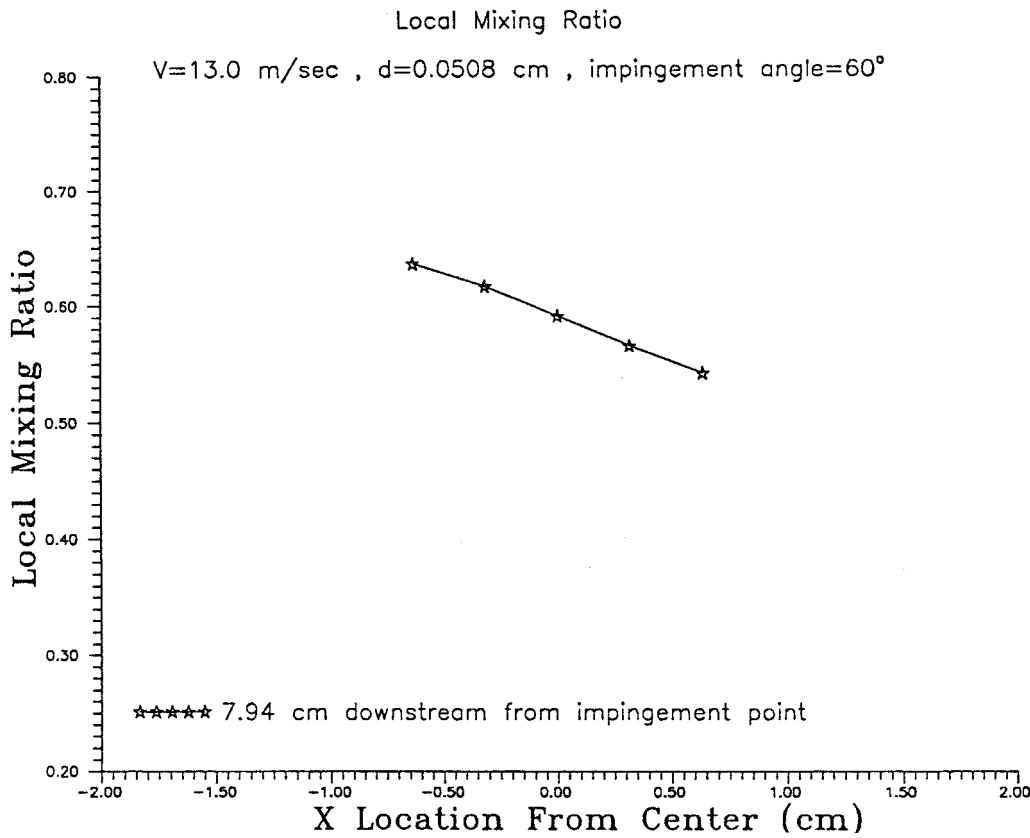
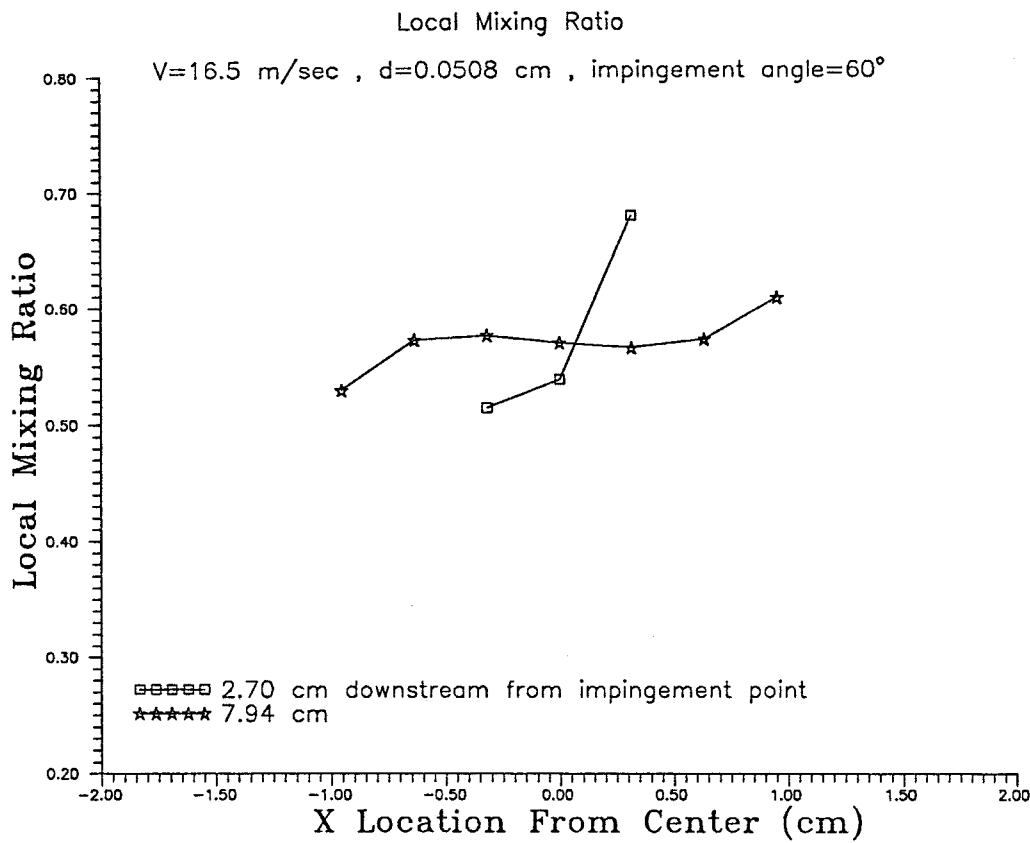


Fig. 5 Variation of local mixture ratio along minor axis of spray for $D_j = 330 \theta \text{ m}$, $Z = 9.21 \text{ cm}$ and $\alpha = 60 \text{ deg}$; shown is transition from reflective atomization to transmissive atomization with increase in jet velocity.

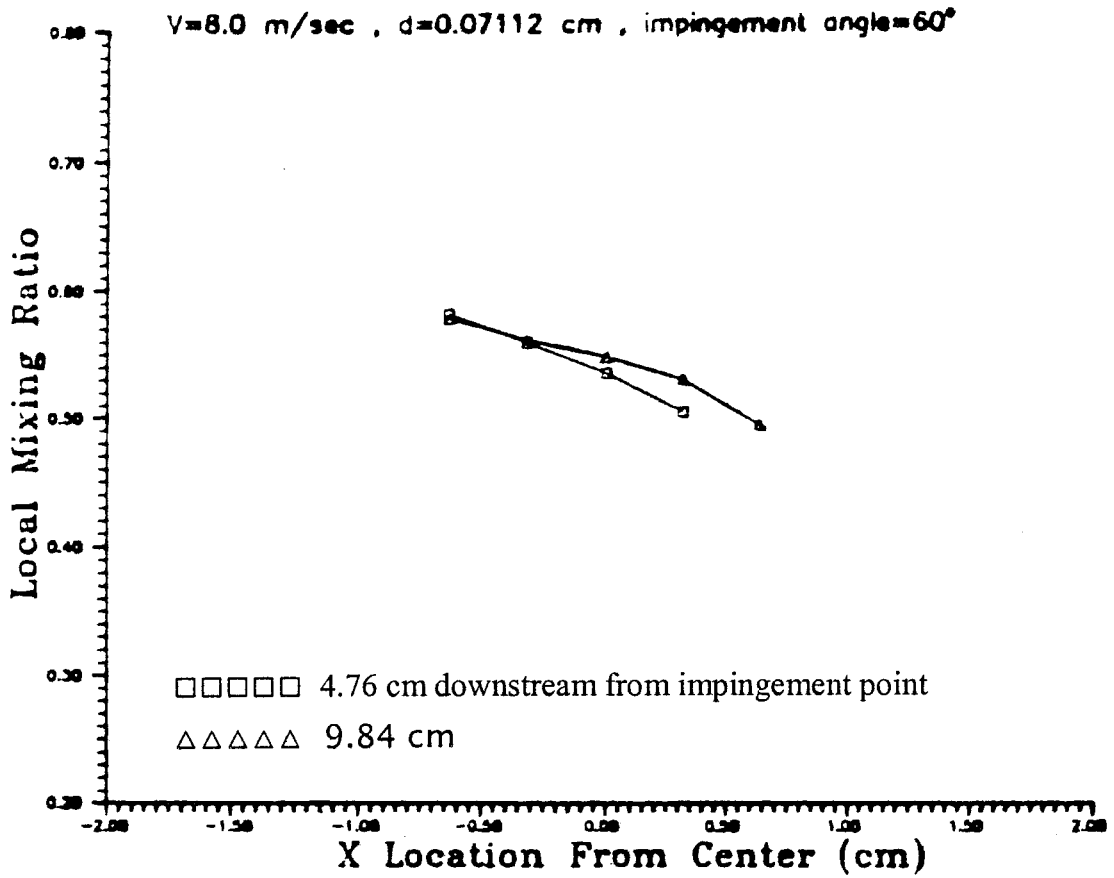


a)

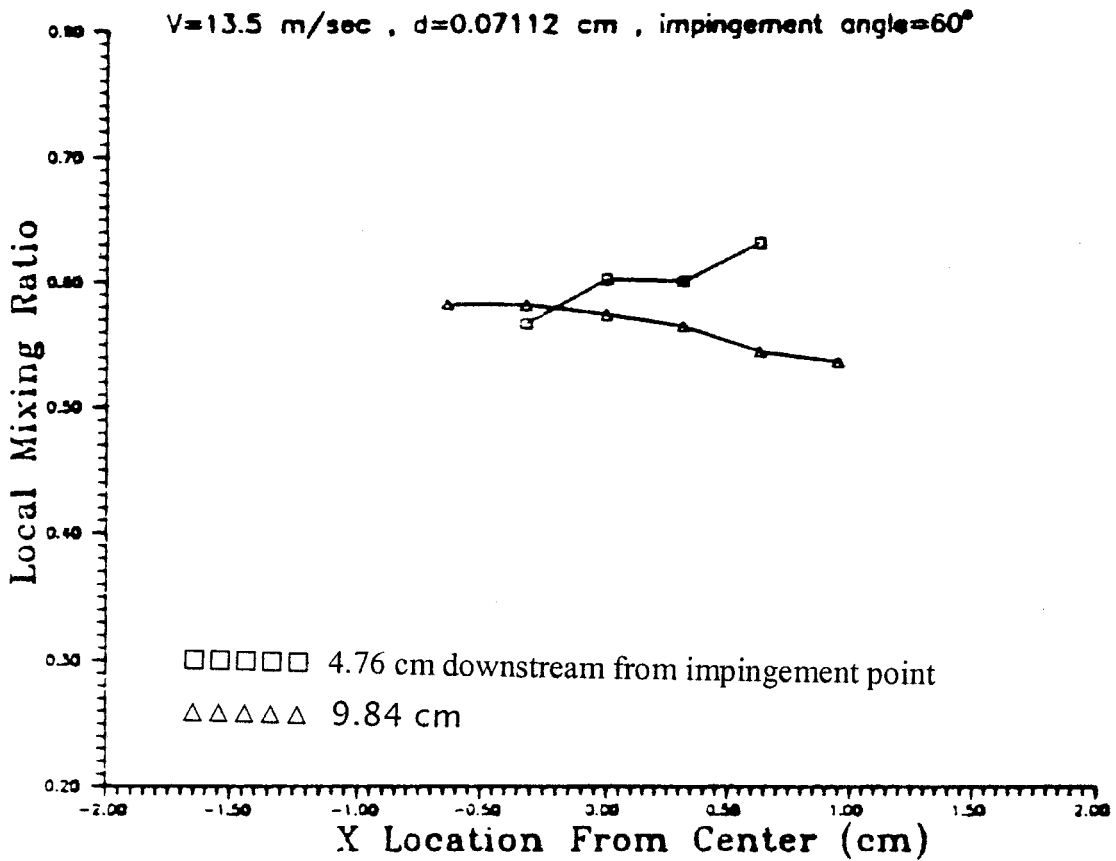


b)

Fig. 6 Variation of the local mixture ratio along the minor axis of the spray for a) $D_j = 508 \theta \text{ m}$, $V_j = 13 \text{ m/s}$, and $\alpha = 60 \text{ deg}$ and b) $D_j = 508 \theta \text{ m}$, $V_j = 16.5 \text{ m/s}$ and $\alpha = 60 \text{ deg}$; shown is influence of jet velocity and mixing along spray length.



a)



b)

Fig. 7 Influence of jet velocity on variation of local mixture ratio along minor axis of spray for a) $D_j = 711 \theta$ m, $V_j = 8$ m/s, and $\alpha = 60$ deg; b) $D_j = 711 \theta$ m, $V_j = 13.5$ m/s and $\alpha = 60$ deg; and c) $D_j = 711 \theta$ m, $V_j = 20$ m/s, and $\alpha = 60$ deg (Continued).

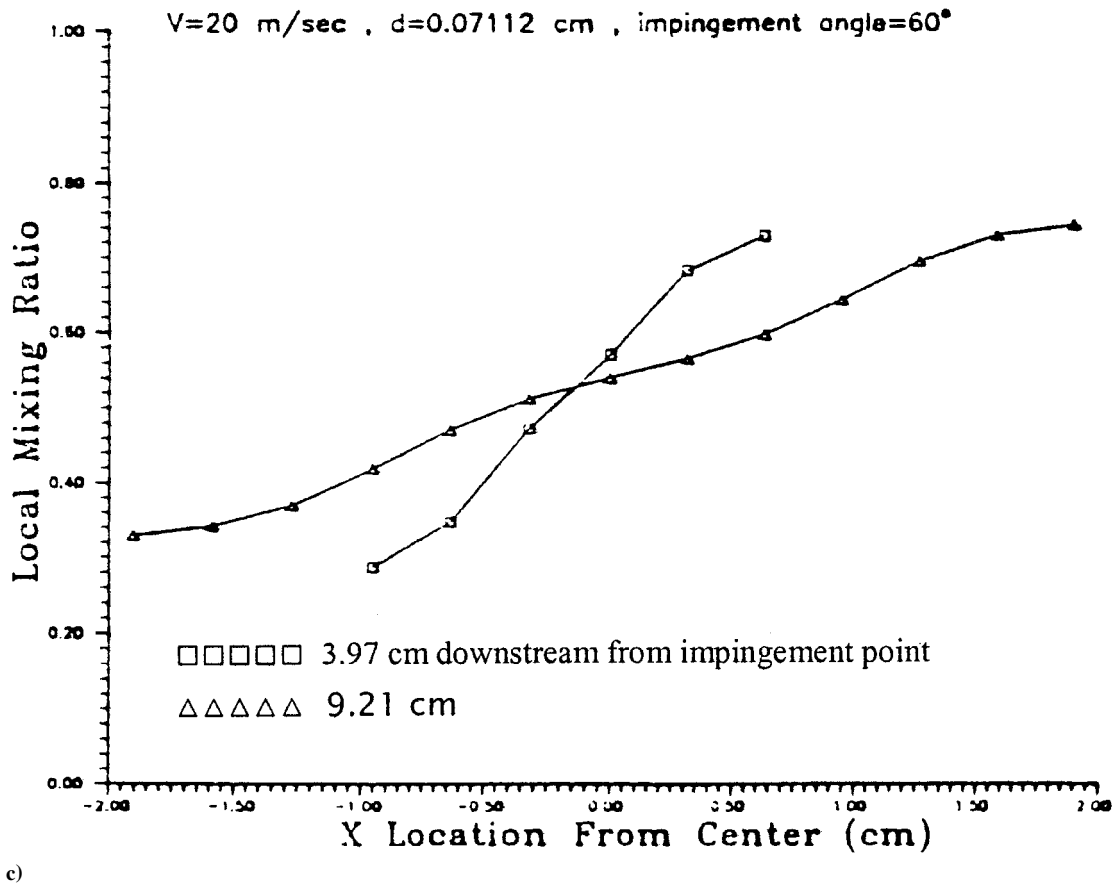


Fig. 7 Influence of jet velocity on variation of local mixture ratio along minor axis of spray for a) $D_j = 711 \text{ }\mu\text{m}$, $V_j = 8 \text{ m/s}$, and $\alpha = 60 \text{ deg}$; b) $D_j = 711 \text{ }\mu\text{m}$, $V_j = 13.5 \text{ m/s}$ and $\alpha = 60 \text{ deg}$; and c) $D_j = 711 \text{ }\mu\text{m}$, $V_j = 20 \text{ m/s}$, and $\alpha = 60 \text{ deg}$.

obtained for jets with larger diameters, for example, $D_i = 508 \text{ }\mu\text{m}$ at $V_i = 13 \text{ m/s}$ of Fig. 6a, and $D_i = 711 \text{ }\mu\text{m}$ at $V_i = 8 \text{ m/s}$ of Fig. 7a. As the jet diameter is increased, the bouncing-type impingement occurs at lower jet velocities.

When the jet velocity is further increased, a totally different distribution of the mixture fraction is obtained. The results indicate that the dyed jet crosses to the side of the undyed jet. This is evident from the plots of mixture fraction in Figs. 5, 6b, 7b, and 7c, where the mixture fraction increases from left to right. Because of the turbulent nature of the flow, there is always some liquid from one jet that transmits to the other side. Therefore, the limiting concentrations of zero and one at the two extremum do not exist.

In general, the experimental results show that, at low jet velocities, the two jets basically bounce off of each other after impingement; however, at high jet velocities, they cross through each other. This can be explained based on the directional momentum of each jet. Consider the impingement of two liquid jets with velocities V_1 and V_2 , and areas A_1 and A_2 , impinging at an angle of α . At low jet velocities, the two jets coalesce after impingement and form a single jet or sheet of liquid. The coalesced jet flows in the direction β (see Fig. 1), which can be determined using a momentum balance:

$$\tan \beta = \frac{V_1^2 A_1 - V_2^2 A_2}{V_1^2 A_1 + V_2^2 A_2} \tan \frac{\alpha}{2}$$

If the momentum of two jets is the same, β will be zero, which means that both jets are equally deflected. However, because of the turbulent nature of the jets, the instantaneous momentum at the time of impingement is not the same, even though the mean momentum of the two jets is the same. This results in the fluctuation of β and, consequently, the fluctuation of the droplet trajectory after the break up of the coalesced jet. In addition, it takes a certain amount of time for the two jets to change direction from their incoming

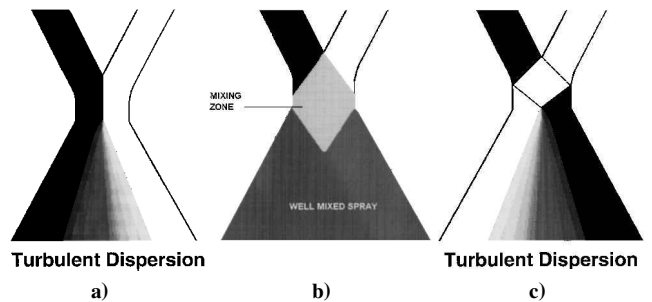
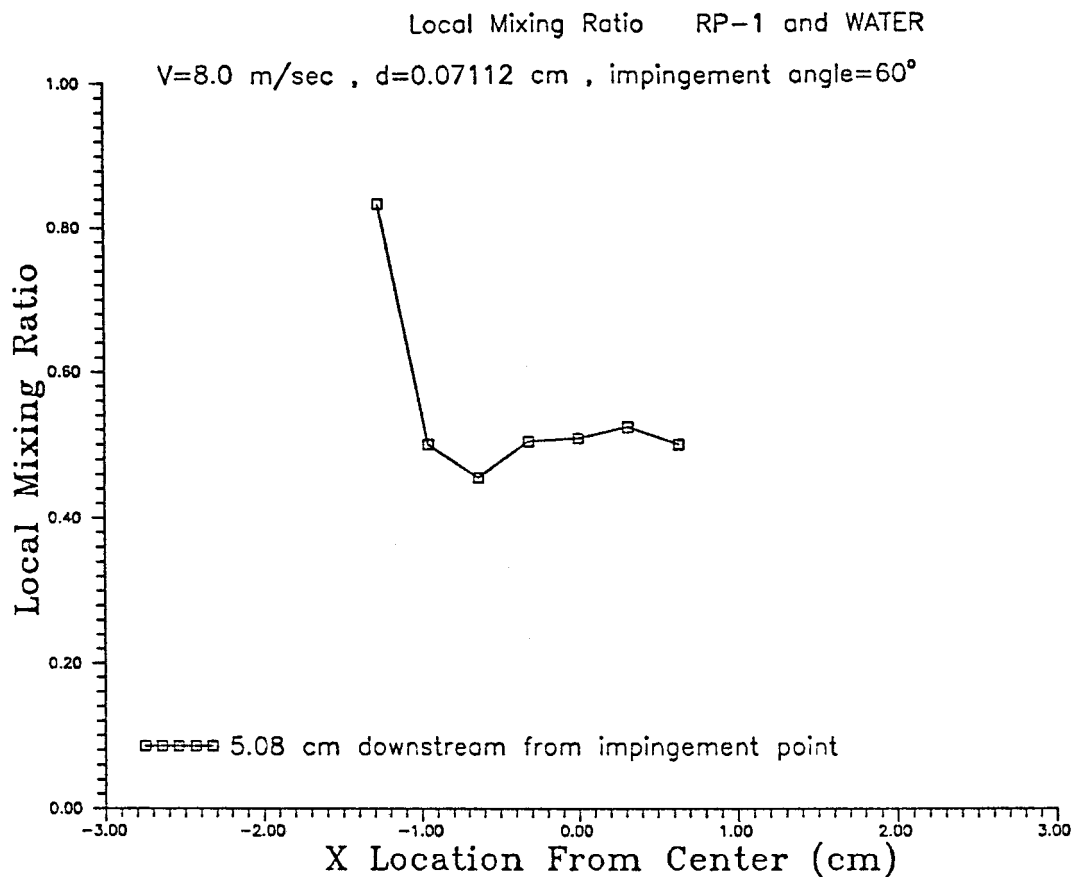


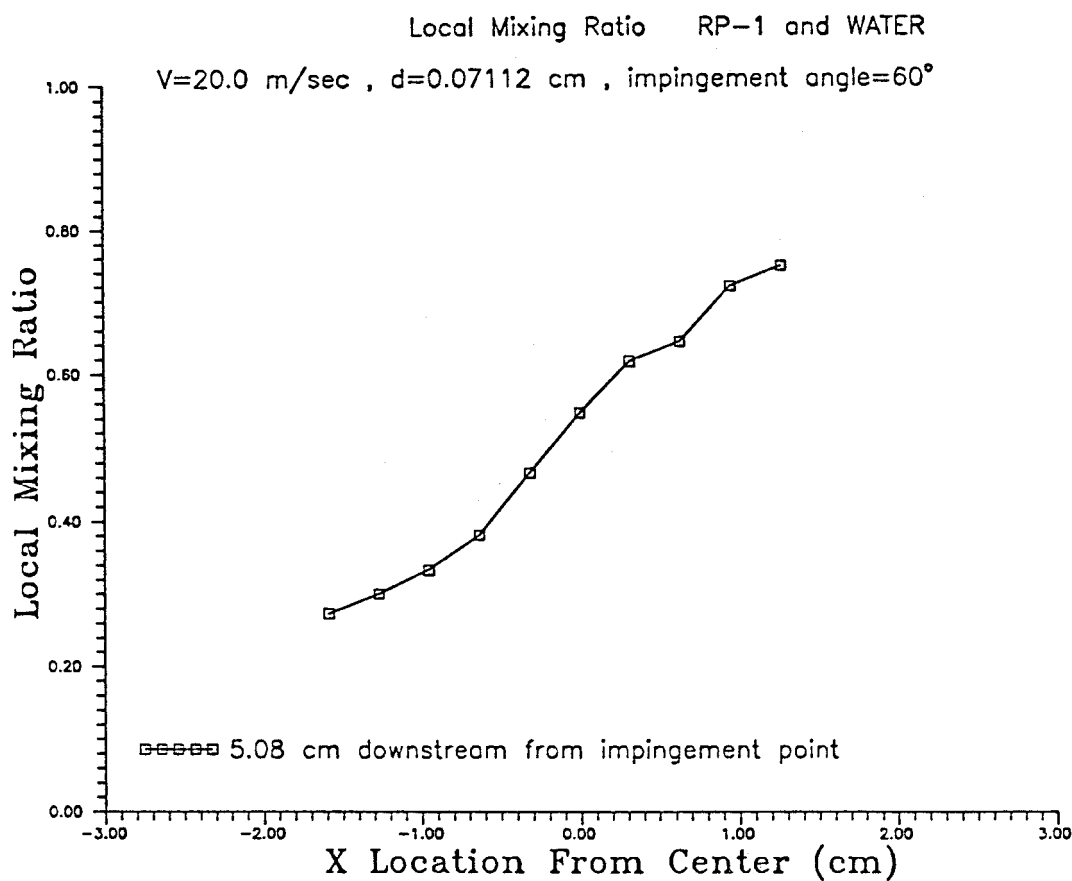
Fig. 8 Schematic of atomization modes: a) reflective, b) well mixed, and c) transmissive atomization; turbulent dispersion downstream of atomization point enhances mixing.

trajectory to the outgoing trajectory with respect to the impingement points. As the velocity of the two jets increases, the coalesced jet (or the liquid sheet) becomes unstable and breaks up into small drops. However, for relatively low velocities, the liquid is redirected in the direction β and the liquid from each jet remains in the same plane after atomization. We call this the reflective type of atomization. A schematic representation of such impingement is shown in Fig. 8a.

As the velocities of the jets are further increased, the coalesced liquid jet or sheet breaks up into droplets after an even shorter amount of time, and the jets do not have time to be completely redirected. After atomization, the trajectory of each drop will be governed by the trajectory of the stream, which has contributed the most to the liquid in that drop. Therefore, shortly after atomization, the drops segregate, and it appears that the two jets cross through each other. We call this the transmissive atomization. Figure 8c shows a schematic of this process. In between the reflective and transmissive atomization lies the optimum well-mixed atomization as depicted in Fig. 8b.

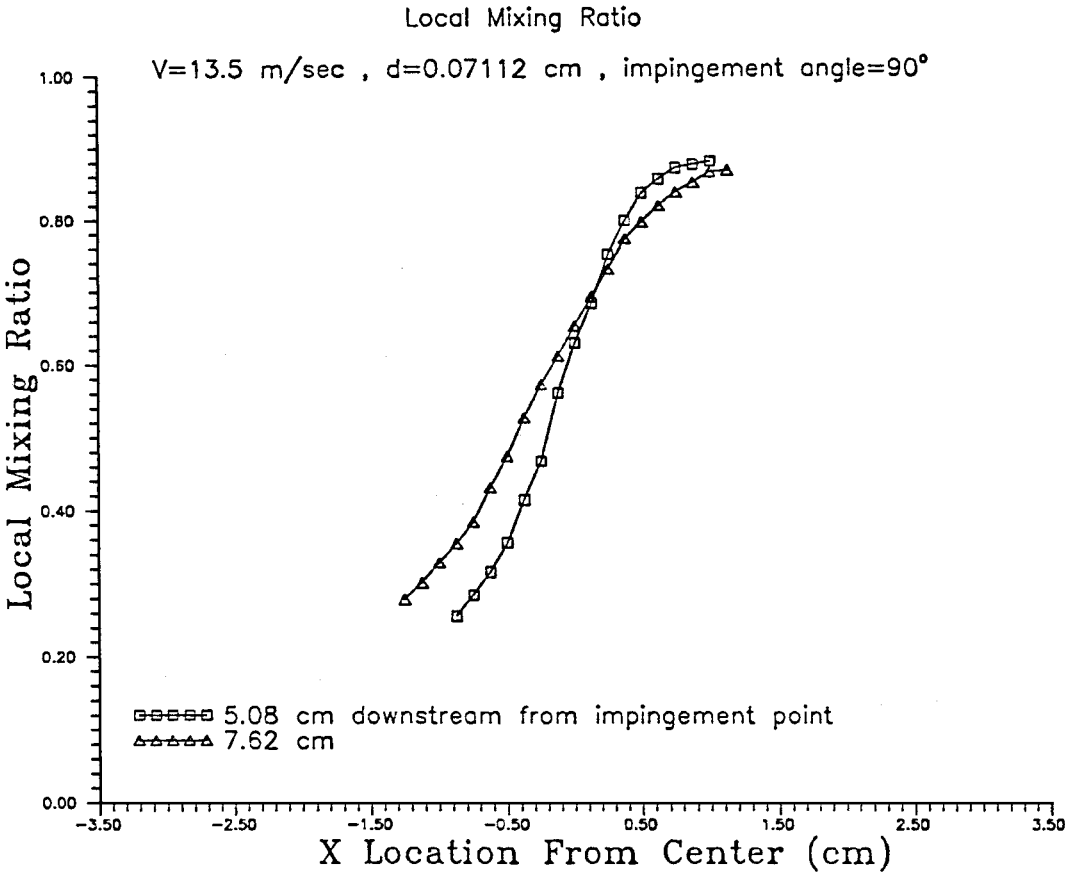


a)

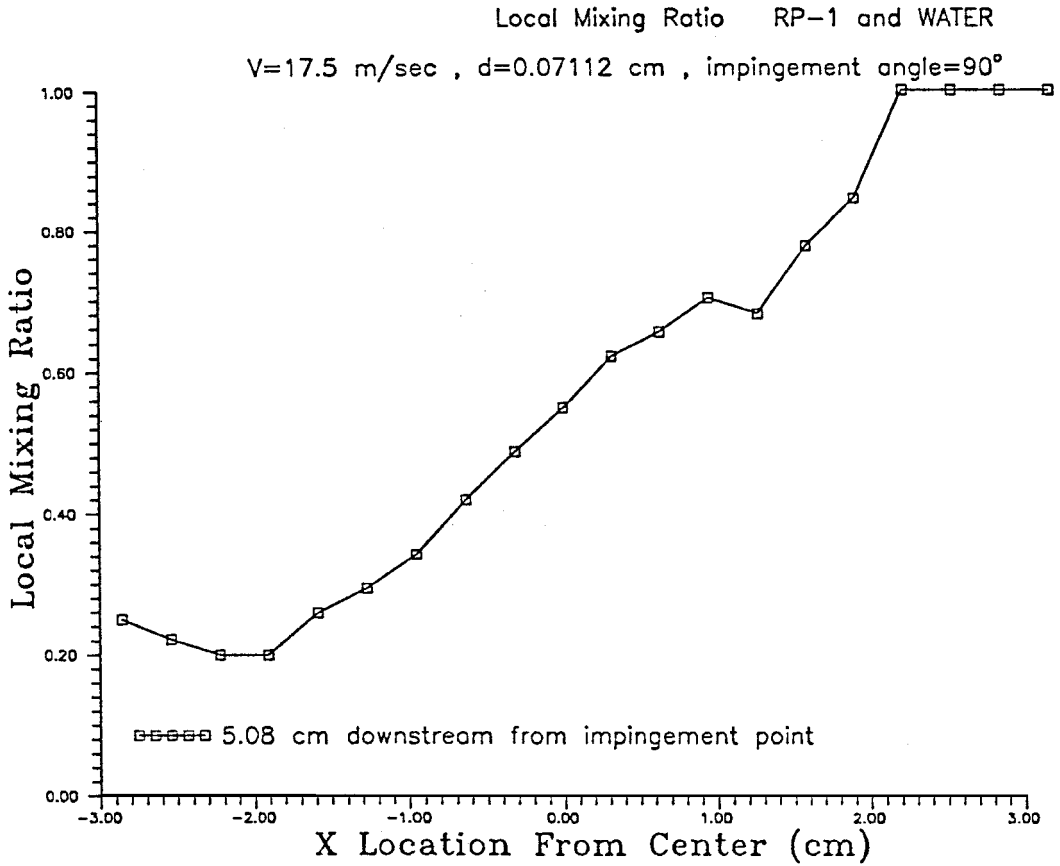


b)

Fig. 9 Impingement results of two immiscible liquid jets of RP-1 and water and for a) $D_j = 711 \mu\text{m}$, $V_j = 8$ m/s, and $\alpha = 60$ deg and b) $D_j = 711 \mu\text{m}$, $V_j = 20$ m/s, and $\alpha = 60$ deg.



a)



b)

Fig. 10 Influence of impingement angle on variation of local mixture ratio along minor axis of spray for a) water jets with $D_j = 711 \theta \text{ m}$, $V_j = 13.5 \text{ m/s}$, and $\alpha = 90 \text{ deg}$ and b) RP-1 and water jets with $D_j = 711 \theta \text{ m}$, $V_j = 17.5 \text{ m/s}$, and $\alpha = 90 \text{ deg}$.

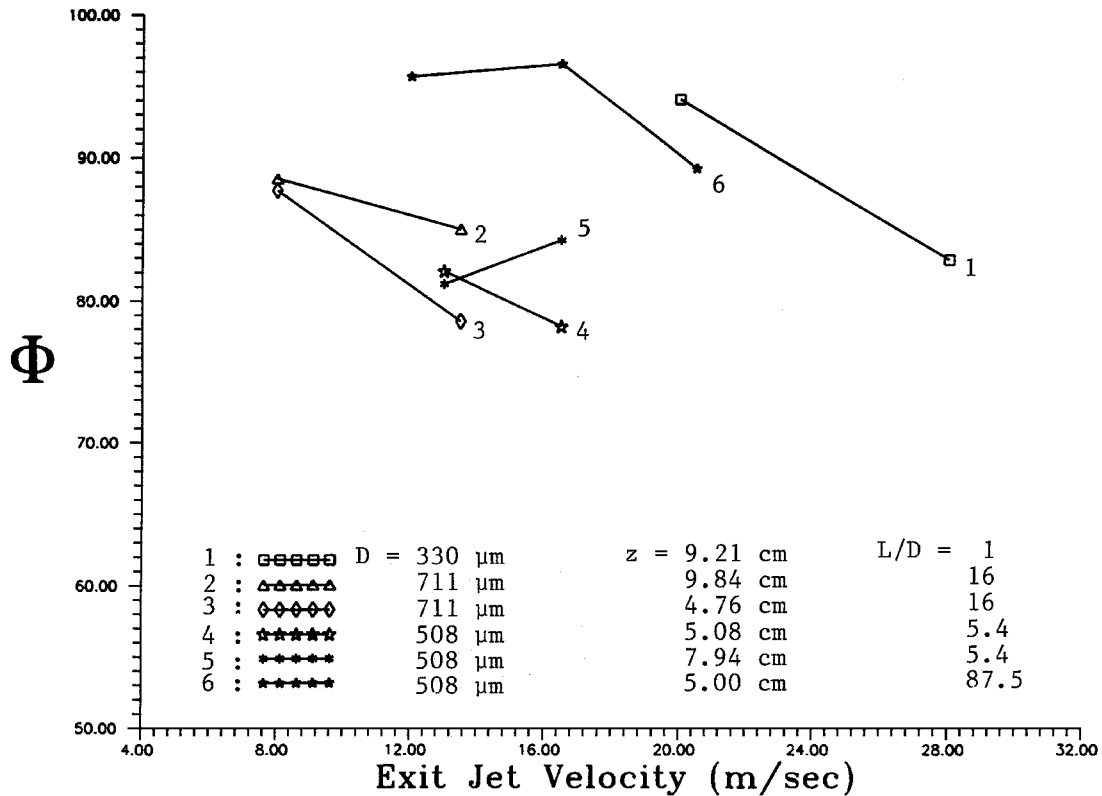


Fig. 11 Variation of extent of mixing with jet velocity for various nozzles.

To achieve proper atomization (relatively small drop sizes), the jets should have high velocities and be turbulent. Therefore, the preceding processes are further complicated by the turbulent nature of the two jets. As was discussed earlier, turbulent liquid jets are not smooth and have many surface fluctuations. The nonsmooth turbulent jets cause the two jets to not collide head-on. Therefore, at the collision point, part of the liquid of each stream that is not interacting with the other stream tends to follow its own initial trajectory. The consequence of this process is the formation of an oscillating and nonsmooth liquid sheet shown in Fig. 4. The parameter that governs the extent of this type of interaction is the amplitude of the surface disturbances at the time of impingement.

The preceding description of the impinging jets explains the experimental observations. Our results show that increasing the jet velocity and/or the impingement angle enhances the liquid crossing. Both the reflective and transmissive atomizations result in poor mixing; however, in the former, the liquid from each stream stays on its own side. In the latter, it crosses to the other side. Therefore, at a certain jet velocity, optimum mixing can occur. In other words, the curves of mixing should show a maximum with jet velocity. However, at low jet velocities, the spray dispersion in the plane of the jets (x axis) was small, and the resolution of our patternator was not sufficient to capture small variations in the jet velocity. Therefore, the results of the reflective atomization are not at sufficiently small velocities, and they are already close to the optimum mixing condition. Any increase from this condition reduces the mixing extent. Generally, higher jet velocities were needed for smaller jet diameters to obtain large enough dispersion in the plane of the jets for accurate measurement of the mixing.

Because almost all of the previous work on mixing in impinging jets has been conducted by using immiscible liquids, we have performed one experiment with such liquids as well, to confirm the general nature of the mixing characteristics described. The results of these experiments are shown in Fig. 9. The two immiscible liquids are water and RP-1. The ratio of the volumes of each liquid in a test tube represents the local mixture fraction. Similar results to the miscible jet impingements are observed: At low jet velocities, the

two jets bounce with minimum mixing as shown in Fig. 9a. Here, the jet on the left is RP-1, and the one on the right is water. As the jet velocity is increased, the two jets cross each other, and a transmissive atomization is observed as shown in Fig. 9b.

The effect of increasing the impingement angle on the mixing is shown in Fig. 10. The experiments are repeated for an impingement angle of 90 deg. Results show that an increase in the impingement angle enhances the transmission; therefore, the extent of mixing reduces. Rupe²¹ had explained this effect by noting that higher impingement angles result in a higher impact-induced turbulence and, therefore, higher turbulence mixing. On the other hand, higher impingement angles will result in smaller contact time between the liquids of the two streams. However, we believe that it is the higher momentum along the spray minor axis that enhances the stream crossing and results in poor mixing.

Plots of mixing extent Φ with the jet velocity, given in Fig. 11, show several effects. If atomization is of the reflective type, an increase in the jet velocity improves the mixing. This is observed on lines 5 and 6 in Fig. 11. As the jet velocity increases, the reflective impingement transforms to transmissive impingement. During this transformation, optimum mixing is achieved at a particular velocity. Curve 6 in Fig. 11 shows an optimum mixing with jet velocity. In the transmissive atomization region the increase in the jet velocity decreases the extent of mixing. The extent of mixing for $D_i = 508 \mu\text{m}$ and at $z = 7.94 \text{ cm}$ (curve 5 in Fig. 11) increases with increasing in V_j . However, similar measurements closer to the injector ($z = 5.08 \text{ cm}$, curve 4 in Fig. 11) show that Φ decreases with increasing V_j . This indicates that the mixing in the post-atomization region plays a significant role in the extent of mixing. The increase in the jet diameter reduces the extent of mixing. This is evident by comparing curve 1 with curves 4 and 5 in Fig. 11.

In addition, the turbulence characteristics of the jet have a significant influence on the extent of mixing. The mixing for the jets with $L/D = 85.5$ (curve 6 in Fig. 11) is much better than that for $L/D = 5.4$ and for the same jet diameter (curves 4 and 5 in Fig. 11). Jets with larger L/D have much smoother surfaces. In the transmissive atomization, the smaller the turbulent fluctuations of the jets

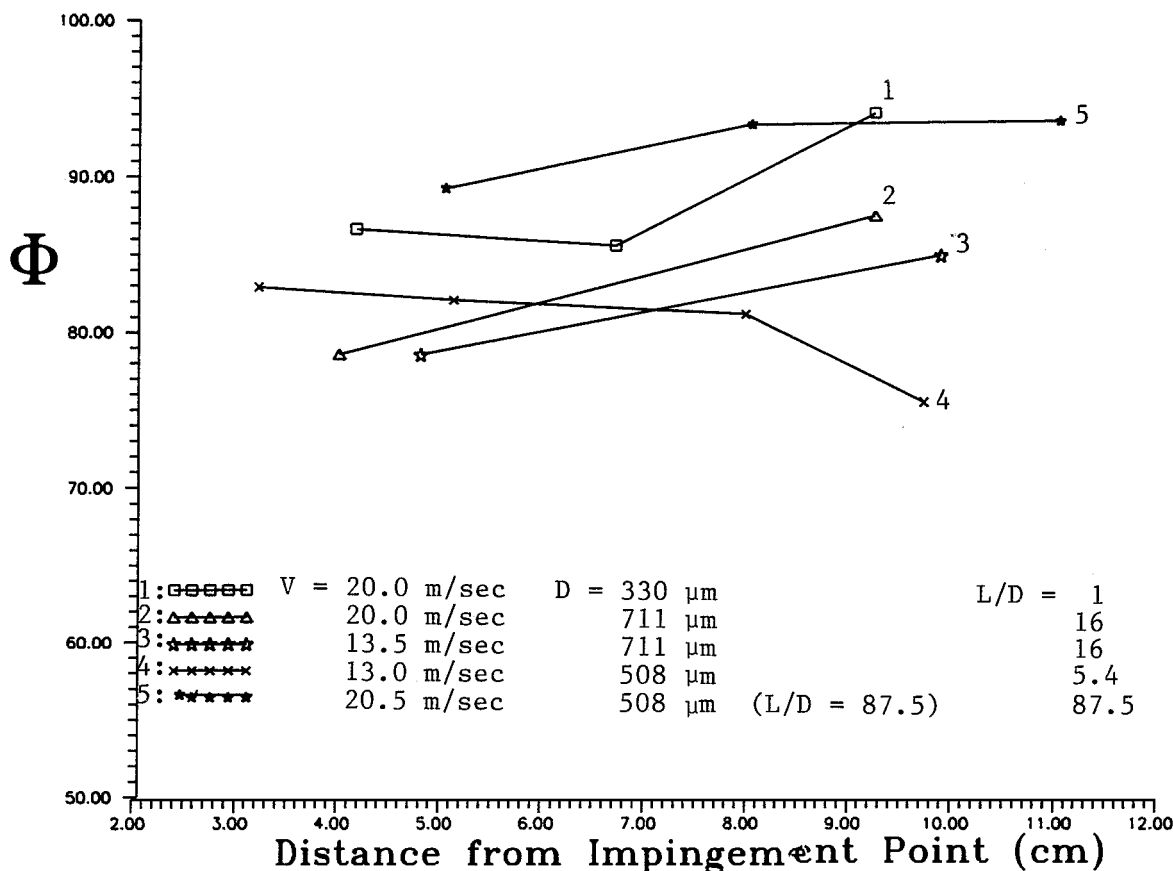


Fig. 12 Variation of extent of mixing along spray length (Z axis) for various nozzles and jet velocities.

before impingement are, the better the mixing is. Note that curves 2 and 3 in Fig. 11 show better mixing results for a jet with a diameter of 711 μ m than those of curves 4 and 5, which belong to a smaller jet diameter of 508 μ m. The reason for the improved efficiency with an increase in the jet diameter in this case is the larger L/D for the larger-diameter jets. The smooth surfaces of the jets compensate for the reduction of the mixing efficiency with an increase in diameter.

In the postatomization region, the turbulent dispersion always improves the mixing. The enhancement of mixing in the postatomization region is better realized by plotting the variation of Φ along the spray axis z , as shown in Fig. 12. In all of the cases, except one, Φ increases downstream of the impingement point. If the jets are significantly segregated by either crossing- or reflecting-type impingement, the segregation increases downstream of the spray. The turbulent dispersion may not be significant enough to compensate for this segregation, and the overall extent of mixing Φ reduces. This effect is shown by curve 4 in Fig. 12 for a pair of jets with $D_i = 508$ μ m and $V_i = 13$ m/s. Generally, in the postatomization region, the turbulent dispersion controls the mixing of the two streams. Therefore, a mixing layer is developed in the central region of the spray, that grows along the spray axis. This explains the observed improvement of the mixing downstream of the impingement point.

V. Concluding Remarks

The mixing process in impinging jet atomizers is controlled by processes in the preatomization and postatomization regions. The preatomization processes control the direction of the final flow of the droplets. At low jet velocities with steady and smooth surfaces, the jets basically bounce off of each other and a reflective type of atomization occurs. As the jet velocity increases, the jets atomize shortly after impingement and do not completely change direction. The result is that the droplets formed from each stream cross to the other side of the impingement plane. This is transmissive atomization. In addition, if the jets are nonsmooth, part of each jet does not interact with the other. The uninteracted part of the jets tends to stretch the

liquid to the other side of the impingement plane, which enhances the transmissive atomization. The extent of jet crossing increases with the jet diameter, jet velocity, and the impingement angle. An increase in the jet velocity, jet diameter, and the impingement angle reduces the time needed to redirect the momentum of each jet. In addition, it increases the amplitude of the surface disturbances and the momentum of the uninteracted region. In the postatomization region the turbulent dispersion develops a mixing layer along the axis of the spray, which enhances the mixing. The overall results can be expressed in terms of the extent of mixing, which may decrease or increase with the jet momentum depending on the type of atomization. The mixing may improve or worsen along the axis of the spray depending on the competition between the turbulent dispersion, which improves the mixing, and the flow separation by the action of the initial reflective or transmissive atomization, which makes the mixing worse.

Most practical impinging jets operate in the parameter range, which results in transmissive atomization. Therefore, in these systems, the extent of mixing decreases with an increase in the jet velocity, jet diameter, and impingement angle. These results are in accordance with the experimental findings of previous investigators cited earlier. In addition, any changes that may result in a more rapid redirection of the jet momentum may improve mixing. Such changes as using elliptical orifices have already proven to improve mixing.²⁶⁻²⁸

Acknowledgments

This work was supported by the Air Force Summer Faculty Research Program. The authors are indebted to Tracy Christensen for superlative technical support.

References

- Heidmann, M. F., and Humphrey, J. C., "Fluctuations in a Spray Formed by Two Impinging Jets," NACA TN 2349, April 1951.

- ²Heidmann, M. F., Priem, R. J., and Humphrey, J. C., "A Study of Sprays Formed by Two Impinging Jets," NACA TN 3835, March 1957.
- ³Rupe, J. H., "A Correlation Between the Dynamic Properties of a Pair of Impinging Streams and the Uniformity of Mixture-Ratio Distribution in the Resulting Spray," Jet Propulsion Lab., Progress Rept. 20-209, California Inst. of Technology, Pasadena, CA, 28 March 1956.
- ⁴Taylor, G. I., "Formation of Thin Flat Sheets of Water," *Proceedings of the Royal Society of London, Series A: Mathematical and Physical Sciences*, Vol. 259, 1960, pp. 1-17.
- ⁵Dombrowski, N., and Hooper, P. C., "A Study of the Sprays Formed by Impinging Jets in Laminar and Turbulent Flow," *Journal of Fluid Mechanics*, Vol. 18, Pt. 3, 1963, pp. 392-400.
- ⁶Fukui, N., and Sato, M., "The Study of a Liquid Atomization by the Impingement of Two Jets," *Bulletin for the Japan Society for Mechanical Engineers*, Vol. 15, 1972, p. 609.
- ⁷Becker, H. A., and Booth, B. D., "Mixing in the Interaction Zone of Two Free Jets," *AIChE Journal*, Vol. 21, 1975, p. 949.
- ⁸Vassallo, P., Ashgriz, N., and Boorady, F. A., "Effect of Flow Rate on the Spray Characteristics of Impinging Water Jets," *Journal of Propulsion and Power*, Vol. 8, No. 5, 1992, pp. 980-986.
- ⁹Anderson, W. E., Ryan, H. M., Pai, S., and Santoro, R. J., "Fundamental Studies of Impinging Liquid Jets," AIAA Paper 92-0458, 1992.
- ¹⁰Ryan, H. M., Anderson, W. E., Pal, S., and Santoro, R. J., "Atomization Characteristics of Impinging Liquid Jets," *Journal of Propulsion and Power*, Vol. 11, No. 1, 1995, pp. 135-145.
- ¹¹Kang, B. S., Shen, Y. B., and Poulikakos, D., "Holography Experiments in the Breakup Region of a Liquid Sheet Formed by Two Impinging Jets," *Atomization and Sprays*, Vol. 5, No. 4-5, 1995, pp. 387-402.
- ¹²Lai, W. H., Huang, W., and Jiang, T. L., "Characteristic Study on the Like-Doubled Impinging Jets Atomization," *Atomization and Sprays*, Vol. 9, No. 3, 1999, pp. 277-289.
- ¹³Arai, M., and Saito, M., "Atomization Characteristics of Jet-to-Jet and Spray-to-Spray Impingement Systems," *Atomization and Sprays*, Vol. 9, No. 4, 1999, pp. 399-417.
- ¹⁴Hasson, D., and Peck, R. E., "Thickness Distribution in Sheet Formed by Impinging Jets," *AIChE Journal*, Vol. 10, No. 10, 1964, p. 752.
- ¹⁵Ibrahim, E. A., and Przekwas, A. J., "Impinging Jets Atomization," *Physics of Fluids A*, Vol. 3, No. 12, 1991, pp. 2981-2987.
- ¹⁶Shen, Y.-B., and Poulikakos, D., "Thickness Variation of a Liquid Sheet Formed by Two Impinging Jets Using Holographic Interferometry," *Transactions of the American Society of Mechanical Engineers*, Vol. 120, Sept. 1998, pp. 482-487.
- ¹⁷Lee, L. J., Ottino, J. M., Ranz, W. E., and Macosko, C. W., "Impingement Mixing in Reaction Injection Molding," *Polymer Engineering and Science*, Vol. 20, 1980, p. 868.
- ¹⁸Tucker, C. L., and Suh, N. P., "Mixing for Reaction Injection Molding. I. Impingement Mixing of Liquids," *Polymer Engineering and Science*, Vol. 20, 1980, p. 875.
- ¹⁹Nguyen, L. T., and Suh, N. P., "Processing of Polyurethane/Polyester Interpenetrating Polymer Networks by Reaction Injection Molding: Part II. Mixing at High Reynolds Numbers and Impingement Pressures," *Polymer Engineering and Science*, Vol. 26, 1986, p. 799.
- ²⁰Mahajan, A. J., and Kirwan, D. J., "Micromixing Effects in Two-Impinging-Jets Precipitator," *AIChE Journal*, Vol. 42, No. 7, 1996.
- ²¹Rupe, J. H., "The Liquid-Phase Mixing of a Pair of Impinging Streams," Jet Propulsion Lab. Progress Rept. 20-195, California Inst. of Technology, Pasadena, CA, 6 Aug 1953.
- ²²Elverum, G. W., Jr., and Morey, T. F., "Criteria for Optimum Mixture-Ratio Distribution Using Several Types of Impinging-Stream Injector Elements," Jet Propulsion Lab., Memorandum 30-5, California Inst. of Technology, Pasadena, CA, 1959.
- ²³Elko, E. R., and Stry, M. L., "Final Report and Design Handbook of Acid-Aniline Rocket Motor and Injector Design," Aerojet Engineering Corp., Rept. 455, Azusa, CA, 9 June 1950.
- ²⁴Hoehn, F., and Rupe, J., "Flow Cavitation Effects on the Mixing Characteristics of Bipropellant Doublets," *8th JANNAF Combustion Meeting*, Vol. 1, Chemical Propulsion Information Agency, Publ. 220, 1971, pp. 569-582.
- ²⁵Nurick, W. H., "Orifice Cavitation and Its Effect on Spray Mixing," *Journal of Fluids Engineering*, Dec. 1976, pp. 681-687.
- ²⁶Mchale, R. M., and Nurick, W. H., "Noncircular Orifice Holes and Advanced Fabrication Techniques for Liquid Rocket Injectors Phase I Final Report," Rocketdyne Div., North American Rockwell Corp., NASA CR-108570, Canoga Park, CA, Oct. 1970.
- ²⁷Mchale, R. M., and Nurick, W. H., "Noncircular Orifice Holes and Advanced Fabrication Techniques for Liquid Rocket Injectors, Comprehensive Program Summary (Phases I, II, III, and IV)," Rocketdyne Div., North American Rockwell Corp., NASA CR-134315, Canoga Park, CA, May 1974, p. 268.
- ²⁸Hoehn, F. W., Rupe, J. H., and Sotter, J. G., "Liquid-Phase Mixing of Bipropellant Doublets," Jet Propulsion Lab., TR 32-1546, California Inst. of Technology, Pasadena, CA, 1972.
- ²⁹Falk, A. Y., and Burick, R. J., "Injector Design Guidelines for Gas/Liquid Propellant Systems," NASA CR-120968, 1968.
- ³⁰Dickerson, R., Tate, K., and Barsic, N., "Correlation of Spray Injector Parameters with Rocket Engine Performance," Rocketdyne Div., TR AFRL-TR-68-147, North American Rockwell Corp., Canoga Park, CA, June 1968.
- ³¹Nurick, W. H., and Clapp, S. D., "An Experimental Technique for Measurement of Injector Spray Mixing," *Journal of Spacecraft and Rockets*, Vol. 6, No. 11, 1969.
- ³²Ferrenberg, A., and Jaqua, V., "Atomization and Mixing Study," Rocketdyne Div., Rept. RI/RD83-170, Rockwell International Corp., Canoga Park, CA, 1983.
- ³³Riebling, R. W., "Criteria for Optimum Propellant Mixing in Impinging-Jet Injection Elements," *Journal of Spacecraft and Rockets*, Vol. 4, No. 6, 1967, pp. 817-819.
- ³⁴Lawver, B. R., "An Experimental Study of the N₂O₄/N₂H₄ Jet Separation Phenomena," *5th ICRPG Combustion Conference*, Chemical Propulsion Information Agency, Publ. 183, 1968, pp. 263-270.
- ³⁵Houseman, J., "Combustion Effects in Sprays," *5th ICRPG Combustion Conference*, Chemical Propulsion Information Agency, Publ. 183, 1968, pp. 255-261.
- ³⁶Johnson, B., "An Experimental Investigation of the Effects of Combustion on the Mixing of Highly Reactive Liquid Propellants," Jet Propulsion Lab., TR 32-689, California Inst. of Technology, Pasadena, CA, 15 July 1965.
- ³⁷Zung, L. B., and White, J. R., "Combustion Process of Impinging Hypergolic Propellants," *7th JANNAF Combustion Meeting*, Chemical Propulsion Information Agency, Publ. 204, Vol. 1, 1971, pp. 455-474.
- ³⁸Hoyt, J. W., and Taylor, J. J., "Waves on Water Jets," *Journal of Fluid Mechanics*, Vol. 83, Paper 1, 1977, pp. 119-127.